THERMAL CYCLING BEHAVIOUR OF PLASMA SPRAYED NiCr-Al-Co-Y_2O_3 BOND COAT IN THERMAL BARRIER COATING SYSTEM

by

Aleksandar A. VENCL[a,b] and Mihailo R. MRDAK[c,*]

[a] University of Belgrade, Faculty of Mechanical Engineering, Belgrade, Serbia
[b] South Ural State University, Chelyabinsk, Russia
[c] Research and Development Center, IMTEL Communications a.d, Belgrade, Serbia

Original scientific paper
https://doi.org/10.2298/TSCI180302374V

The aim of this study was to investigate the thermal cycling behaviour of NiCr-Al-Co-Y_2O_3 bond coating in thermal barrier coating system with ZrO_2-MgO as a top coating. The coatings were deposited by atmospheric plasma spraying on stainless steel X15Cr13 (EN 1.4024) substrate. The used composite powder NiCr-Al-Co-Y_2O_3 was mechanically cladded, and the steel substrates were preheated to 160-180 °C. The thermal cycling performance of the obtained bond coat and the effect of formed complex ceramic oxides of the Al_2O_3-Y_2O_3 system were tested by heating to 1200 °C and cooling in air to 160-180 °C. The number of performed thermal cycles was 7, 32, and 79. The quality of the obtained coating, as well as its thermal cycling behaviour, was assessed through the microstructural analysis, microhardness and tensile bond strength measurements, and change in chemical composition and microhardness. The obtained results showed that the steel substrate, bond coat oxidation and interdiffusion at bond coat/substrate interface have a significant influence on changes in chemical composition and microhardness of the bond coat. The correlation between oxidation behaviour of NiCr-Al-Co-Y_2O_3 bond coat and number of thermal cycles was also discussed.

Key words: *thermal barrier coating, NiCr-Al-Co-Y_2O_3 bond coat, atmospheric plasma spraying, oxidation behaviour, thermal cycling*

Introduction

Thermal barrier coatings (TBC) find increasing application in the most demanding high temperature environment of aircraft and industrial engines. They are widely applied to protect the hot-section components of gas turbine engines [1-3], combustion chambers of internal combustion engines [4, 5], and in other industries. Typical TBC systems consist of a yttria stabilized zirconia (YSZ) ceramic top coat layer, with low thermal conductivity to provide thermal insulation, and a metallic MCrAlY (where M = Ni and/or Co) bond coat, which improves bonding between the substrate and the top coat and protects the substrate from corrosion and oxidation. In such two-layered TBC systems, a thin thermally grown oxide (TGO) layer always forms at the surface of the bond coat, because the YSZ is a porous layer, transparent to oxygen at high temperatures [6]. The TGO layer prevents oxygen from entering the bond coat and protects the bond coat and substrate from oxidation.

The TGO layer plays an important role in TBC performance. One of the main reasons for the failure of TBC systems exposed to thermal cycling is delamination of ceramic top coat

* Corresponding author, e-mail: drmrdakmihailo@gmail.com

[7, 8].This failure is caused by the crack of TGO layer, which is driven by oxidation-induced volume increase of the TGO or by differences in the coefficient of thermal expansion between TGO and bond coat [6]. There are at least four primary failure mechanisms in atmospheric plasma sprayed (APS) TBC systems exposed to thermal cycling: cracking at the bond coat/TGO interface at TGO crests, fracture along the TGO/top coat interface at the TGO crests, cracking within the highly brittle top coat in the vicinity of the TGO crests, and cracking within the top coat in the 'valleys' between the TGO crests [9].

The oxidation behaviour of the bond coat depends on its composition and microstructure, and the thickness of TGO layer (which is in direct correlation with the bond coat composition, working temperature and time of exposure to high temperature oxidation). With typical bond coats, *i.e*. NiCrAlY and NiCoCrAlY alloys, in the transient stage of oxidation, *i.e*. before a continuous TGO layer has been formed and during which all oxide-forming species in the alloy (Ni, Co, Cr, Al, *etc*.) might form oxides, various oxides are formed (NiO, CoO, Cr_2O_3, $NiAl_2O_4$, $NiCr_2O_4$, α-Al_2O_3, *etc*.) [10-12]. In the following steady-state stage of oxidation, one oxidising species becomes dominant and forms a continuous TGO layer on the bond coat surface. Different TGO layer oxides meet the requirement of resistance to high temperature oxidation. In general, Cr_2O_3 is ideal against oxidation below 1000 °C and Type II hot corrosion (700-800 °C), and Al_2O_3 (particularly in its α phase form) is the best against high temperature oxidation above 1000 °C and Type I hot corrosion (800-950 °C) [6].

In the tested composite bond coat NiCr-Al-Co-Y_2O_3, ductile complex ceramic oxides of the Al_2O_3-Y_2O_3 dual system are also present in the as-deposited condition. In the Al_2O_3-Y_2O_3 system, there are three important compounds, *i.e*. yttrium aluminium garnet (YAG), yttrium aluminium perovskite (YAP) and yttrium aluminium monoclinic (YAM) [13]. Since the used powder was composite, manufactured by a mechanical cladding method, most of aluminium during deposition reacts with oxygen and yttria (and form Al_2O_3-Y_2O_3 compounds), thus minimising diffusion of aluminium on the bond coat surface and formation of α-Al_2O_3 TGO layer during exploitation. The formed Al_2O_3-Y_2O_3 compounds are more ductile than α-Al_2O_3, so it is more resistant to stresses brought about by thermal expansion mismatch between the ceramic top coat and metal bond coat. These complex ceramic oxides are also stable on the temperature above 1200 °C. Surprisingly, the NiCr-Al-Co-Y_2O_3 coating is not represented in the literature adequately, although it is obtained by depositing a commercial powder. In the present paper, the oxidation behaviour of NiCr-Al-Co-Y_2O_3 bond coat and the effect of complex ceramic oxides of the Al_2O_3-Y_2O_3 system were evaluated through the thermal cycling at 1200 °C.

Experimental details

Materials and spray conditions

Substrate material was stainless steel X15Cr13 (EN 1.4024), used without any heat treatment. Two spray powders were used to produce the TBC system, *i.e*. Metco 461 NiCr-Al-Co-Y_2O_3 composite powder for the bond coat, and Metco 210 ZrO_2-MgO powder for the top coat. The NiCr-Al-Co-Y_2O_3 powder particles have been manufactured by a mechanical cladding method. In this method NiCr alloy particles size from 40 to 50 μm were used as a core. These core particles were usually obtained by a dry spraying or by atomization of liquid melt with inert gas. Cladding of the core NiCr particles was done with small particles (size from 1 to 10 μm) of Al, Co, and Y_2O_3, with the use of suitable organic binders. Manufacturing of composite powder by cladding method allows the exothermic reaction between the powder components during deposition. The realised heat energy provided better metallurgical bonding of the coating to the metal substrate. Chemical composition of the powder used in experiment is shown in tab.1, and

its morphology in fig. 1. The SEM shows that the powder particles are with rounded edges and have irregular morphology. The powder grain size range was: – 150 + 45 μm.

Table 1. Chemical composition of NiCr-Al-Co-Y_2O_3 powder (wt. %)

Element	Cr	Al	Co	Y_2O_3	Ni
Percentage	17.5	5.5	2.5	0.5	Balance

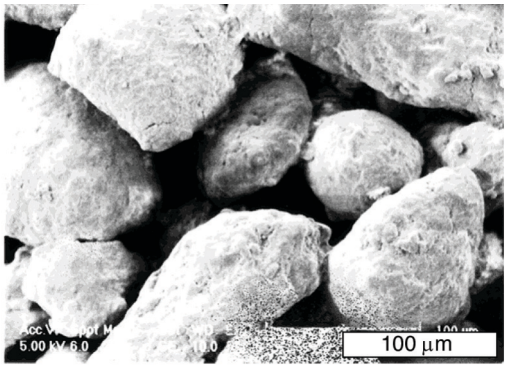

Figure 1. Morphology (SEM) of NiCr-Al-Co-Y_2O_3 powder particles

The ZrO_2-MgO powder is oxide powder composed of ZrO_2 (76 wt.%), which is stabilized with MgO (24 wt.%). Coatings of magnesia stabilized zirconia powders have low thermal conductivity and are suitable for particle erosion in high temperatures. The ZrO_2-MgO powder particles have been manufactured by fusing and subsequent crushing, so the powder particles are with sharp edges and have irregular morphology. The powder grain size range was: – 53 + 10 μm. Some thermophysical properties, given by the manufacturers, of the substrate and obtained coatings are shown in tab. 2.

Table 2. Thermophysical properties at ambient temperature of substrate and obtained coatings [14,15]

Material	Thermal conductivity [W/mK]	Coefficient of linear thermal expansion [m/mK]
Steel substrate	30	11×10^{-6}
NiCr-Al-Co-Y_2O_3 coating	23-28	13×10^{-6}
ZrO_2-MgO coating	1-1.5	11×10^{-6}

The APS, with Plasmadyne SG-100 plasma spray gun, was utilized in the experiment. Argon combined with helium was used as a plasma gas, and electric current of 900 A and 38 V was used for both coatings deposition. Before the spraying process, the surface of the steel substrate was activated and preheated. Activation (roughening) was done with white fused alumina (Al_2O_3) using particle sizes of 700-1500 μm. Before the deposition, the substrate was preheated to 160-180 °C. The bond coat (NiCr-Al-Co-Y_2O_3), with a thickness range of 68-85 μm, was produced in a single pass of a spraying gun (one layer), while the top coat (ZrO_2-MgO), with a thickness range of 500-550 μm, was obtained after fifteen passes of a spraying gun. The other spray parameters are summarised in tab. 3. Since the thermal cycling behaviour was investigated after three different numbers of cycles, three sets of samples were produced for each testing, *i.e.* for microstructural analysis, for microhardness and tensile bond strength characterisation, and for thermal cycling testing.

Table 3. APS spray parameters values used for coating deposition

Spray parameter	Coating	
	Bond coat	Top coat
Primary plasma gas (Ar) [l/min]	47	47
Secondary plasma gas (He) [l/min]	12	12
Powder carrier gas (Ar) [l/min]	5	7
Powder feed rate [kg/h]	3.6	3.0
Spray distance [mm]	115	100
Traverse speed [mm/s]	250	250

Microstructural and mechanical characterization

Microstructural and mechanical (microhardness and tensile bond strength) characterization of the obtained TBC samples was done according to Pratt & Whitney manual [16]. For the

metallographic examination and hardness measurement specimens 70 × 20 × 1.5 mm were used, while for the tensile bond strength measurement cylindrical specimens Ø25 × 50 mm were used.

Microstructural characterisations were performed on coatings cross-section by means of optical microscopy (OM), SEM, and energy dispersive spectrometry (EDS). Metallographic specimens were prepared in a standard way applying grinding and polishing. Polished specimens were used for the SEM/EDS analysis, whereas specimens for OM examinations were polished or etched with $1HNO_3$:4HCl:$4H_2O$ solution.

Microhardness measurements were carried out using a Vickers diamond pyramid indenter and 100 g load (HV 0.1) before and after thermal cycling testing. Measurement was carried out in the direction along the lamellae on three places on the coating cross-section, *i.e.* in the middle and at the ends of the specimen. Five measurements were made on each place in order to eliminate possible segregation effects and to obtain a representative value of the coating microhardness. The presented values are the average ones.

Tensile bond strength measurements were performed at room temperature on a hydraulic tensile test rig using a cross-head speed of 10 mm per minute. The bond strength was calculated by dividing the failure load by the cross-sectional area of the specimen. The geometry of the specimens was according to ASTM C633 standard. Two specimens in a pair were used, and the coating was deposited only on one of them. Specimens were bonded by glue and kept pressed against each other in a furnace at temperature of 180 °C for 2 hours. For each test sample, measurements were repeated three times, and the results werve averaged.

Thermal cycling testing

In order to evaluate the thermal cycling performance of the obtained bond coat and the effect of the complex ceramic oxide Al_2O_3-Y_2O_3, laboratory thermal cycle testing was conducted in a programmable, automated furnace. Specimens for testing were made by pairing two TBC samples, and placing metal plate with a thermocouple between them. This thermocouple measured the temperature on the lower surface of the substrate. The other thermocouple was placed on the top coats surface and measured their temperatures. Detailed description of the equipment and measurement method is presented elsewhere [7].

Thermal cycling testing was done in the condition of cyclic intermittent heating and cooling of the samples. Rapid heating of the samples was to the temperature of 1200 °C, and rapid cooling was to the temperature between 160 and 180 °C. Each thermal cycle consisted of heating for 2 minutes and forced air cooling for 3 minutes. Three sets of samples (sample 1, sample 2, and sample 3) were tested for different number of thermal cycles, *i.e.* the number of performed thermal cycles for sample 1, sample 2, and sample 3 was: 7, 32, and 79, respectively. After thermal cycling testing, microhardness measurements and microstructure SEM/EDS analysis were performed for each sample, and compared with the condition before thermal cycling testing.

Results and discussion

Microstructure

The microstructures of all three tested samples (sample 1, sample 2, and sample 3) were similar. Typical microstructure of as-deposited TBC system (NiCr-Al-Co-Y_2O_3 bond coat and ZrO_2-MgO top coat) is shown in fig. 2. Both coatings showed uniform lamellar structure with negligible amount of unmelted particles. Presence of micro and macro cracks on both interface (between substrate and bond coat and between bond and top coat) was not noticed, *i.e.* there is no peeling of the TBC from the substrate. Presence of cracks in both coatings was not noticed also. All this resulted in relatively high microhardness and tensile bond strength values, as presented in section *Mechanical properties*.

The as-deposited NiCr-Al-Co-Y_2O_3 bond coat contains lamellar nickel-chrome particles surrounded by thin oxide structures, essentially Al_2O_3 and Al_2O_3-Y_2O_3 [14]. The base of the nickel-chrome lamellae consists of a γ-Ni(Cr) solid solution. Pores, interlamellar porosity, thin lamellar α-Al_2O_3 oxides and complex oxides $YAlO_3$ (YAP) and $Y_3Al_5O_{12}$ (YAG) of the Al_2O_3-Y_2O_3 dual system [17] are arranged between the nickel-chrome lamellas. This thin oxide lamellas are evenly distributed on the boundaries of nickel-chromium lamellas, which indicates that at some places in the coating, the γ-Ni(Cr) solid solution lamellas are surrounded with oxides and protected from further oxidation.

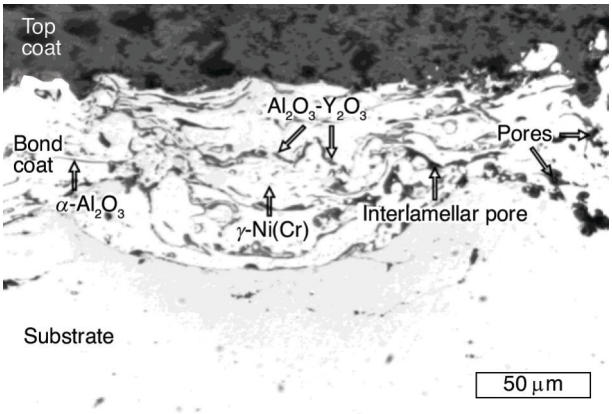

Figure 2. Microstructure (OM, polished) of the as-deposited NiCr-Al-Co-Y_2O_3 / ZrO_2-MgO TBC system (sample 3)

The EDS analysis of the as-deposited NiCr-Al-Co-Y_2O_3 bond coat is performed on SEM image, fig. 3. It could be noticed that the chemical composition of as-deposited NiCr-Al-Co-Y_2O_3 coating differs from the chemical composition of NiCr-Al-Co-Y_2O_3 powder, tab. 1. This change is expected as a result of Al oxidation and exothermic reaction amongst Al and Co during the deposition. The smaller amount of Al in the γ-Ni(Cr) solid solution lamellas (EDS on fig. 3) indicates that most of the Al reacted with oxygen from the air and with Y_2O_3 from the powder, during the deposition. The primary Al_2O_3 oxide is formed due to the oxidation of Al, *i.e.* $4Al + 3O_2 \rightarrow 2Al_2O_3$. The molten aluminium also reacts with molten yttrium oxide and forms the $YAlO_3$ (YAP) phase in the reaction: $3Al + Y_2O_3 \rightarrow YAlO_3 + Al_2Y$. The reaction between YAP phase and Al_2O_3 forms $Y_3Al_5O_{12}$ (YAG) phase, *i.e.* $3YAlO_3 + Al_2O_3 \rightarrow Y_3Al_5O_{12}$. The YAG phase can also be formed directly due to the reaction: $5Al_2O_3 + 3Y_2O_3 \rightarrow 2Y_3Al_5O_{12}$ [17, 18].

All this minimise the diffusion of aluminium on the bond coat surface at 1200 °C, and formation of more brittle α-Al_2O_3 TGO layer. The formed complex oxides of the Al_2O_3-Y_2O_3 system are more ductile than α-Al_2O_3, so the formed coating should be more resistant to cracking during the thermal cycling testing.

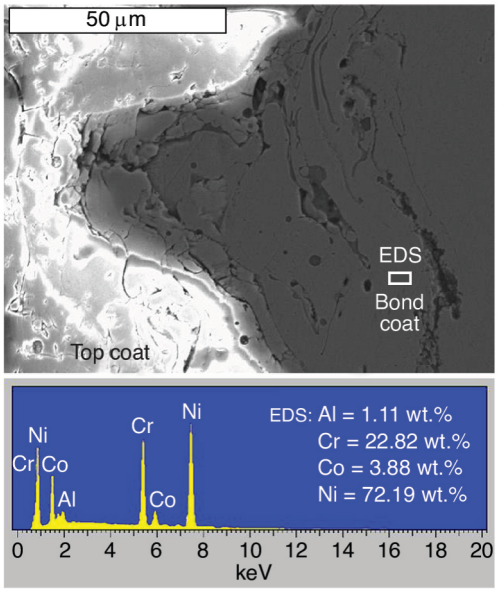

Figure 3. Microstructure (SEM, polished) of the as-deposited NiCr-Al-Co-Y_2O_3 / ZrO_2-MgO TBC system (sample 3) and corresponding EDS analysis results

Mechanical properties

The obtained values of microhardness for bond coat (NiCr-Al-Co-Y_2O_3) samples, before and after thermal cycling testing, are shown in fig. 4. Microhardness values obtained after the testing were shown together with room-temperature

values (before the testing) for the purpose of easier comparison, and will be discussed in section *Thermal cycling behaviour*. As expected, microhardness values measured before the thermal cycling testing were similar for different samples of the same coating. There are some differences, but they were in acceptable range, *i.e.* below 9%. Nevertheless, all samples had relatively high starting microhardness, *i.e*. higher than the expected limits for this type of coating (HV 0.3 = 200-225) [14]. The main reason for relatively high starting microhardness values is the preheating of the substrate, which is discussed in more detail elsewhere [7].

The obtained values of tensile bond strength for bond coat (NiCr-Al-Co-Y_2O_3) samples, before thermal cycling testing, are shown in tab. 4. The values for different samples of the same coating were very similar (in the range 52-54 MPa), and higher than the expected limits for this type of coating (31.0-34.4 MPa) [14]. The main reason for relatively high tensile bond strength values is also the preheating of the substrate [7]. The obtained values are in correlation with the obtained bond coat microstructure. They are also in correlation with the microhardness values measured before the thermal cycling testing, *i.e*. samples with higher microhardness show higher tensile bond strength and vice versa. For all three samples, the type of failure that occurred during the tensile bond strength characterization was adhesive, *i.e*. the fracture occurred through the bond coat/substrate interface [19]. This means that the adhesive strength of bond coat/top coat interface and the cohesive strength of both TBC layers are good, *i.e*. higher than the adhesive strength of bond coat/substrate interface.

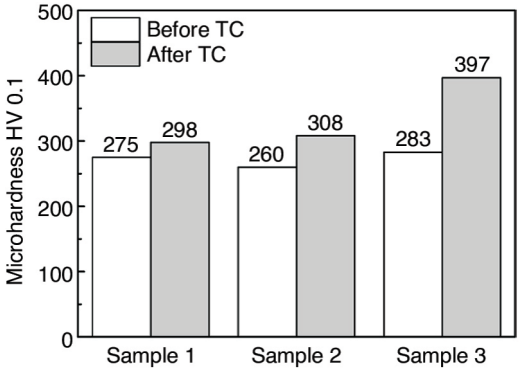

Figure 4. Average microhardness values of bond coat (NiCr-Al-Co-Y_2O_3) samples before and after thermal cycling (TC) testing

Table 4. Average tensile bond strength values of bond coat (NiCr-Al-Co-Y_2O_3) samples before thermal cycling testing

Bond coat sample	Tensile bond strength [MPa]
Sample 1	53
Sample 2	52
Sample 3	54

Thermal cycling behaviour

Metallographic analysis, figs. 5 and 6, of the NiCr-Al-Co-Y_2O_3 / ZrO_2-MgO TBC system after thermal cycling testing showed generally good oxidation resistance of the NiCr-Al-Co-Y_2O_3 bond coat. Thermal cycling testing at 1200 °C affected the bond between bond coat and substrate, but the delamination of the coating, *i.e*. the type of failures that usually occur during the exploitation, was not noticed on any sample, fig. 5. The microstructure of the ceramic ZrO_2-MgO top coat shows the presence of horizontal (parallel and close to the bond coat/top coat interface) and vertical cracks (through the top coat). These cracks are the result of the high thermal stress during the process of cyclic heating and cooling of the samples (thermal cycling testing), and to some extent the stresses brought about by thermal expansion mismatch between the ceramic top coat, metal bond coat and substrate.

Figure 6 shows martensite structure of the steel substrate and presence of oxides in the bond coat. The amount of these oxides is higher, comparing to the as-deposited condition, and it becomes higher as the number of thermal cycles increase. However, formation of the brittle TGO layer was not noticed, not even in the sample 3, *i.e*. after 79 cycles. The ceramic ZrO_2-MgO

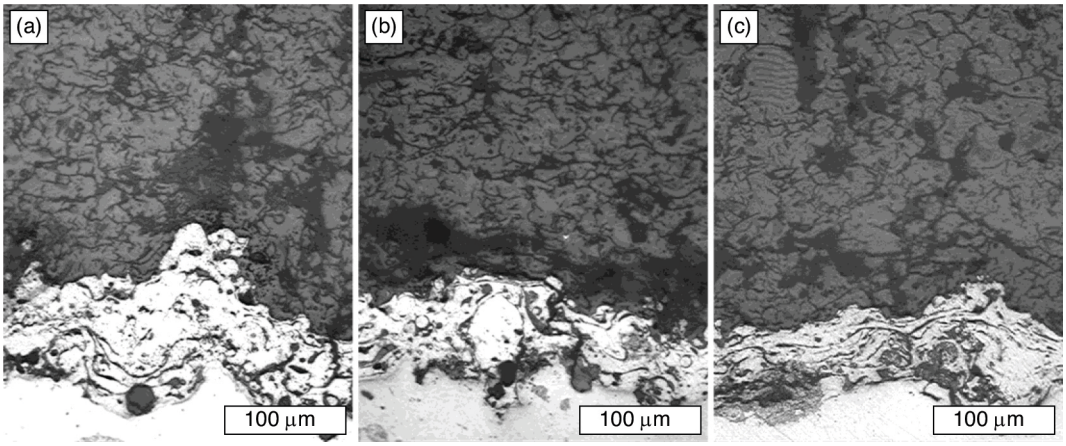

Figure 5. Microstructure (OM, polished) of the NiCr-Al-Co-Y_2O_3 / ZrO_2-MgO TBC system after thermal cycling testing; (a) sample 1 (after 7 cycles), (b) sample 2 (after 32 cycles), and (c) sample 3 (after 79 cycles)

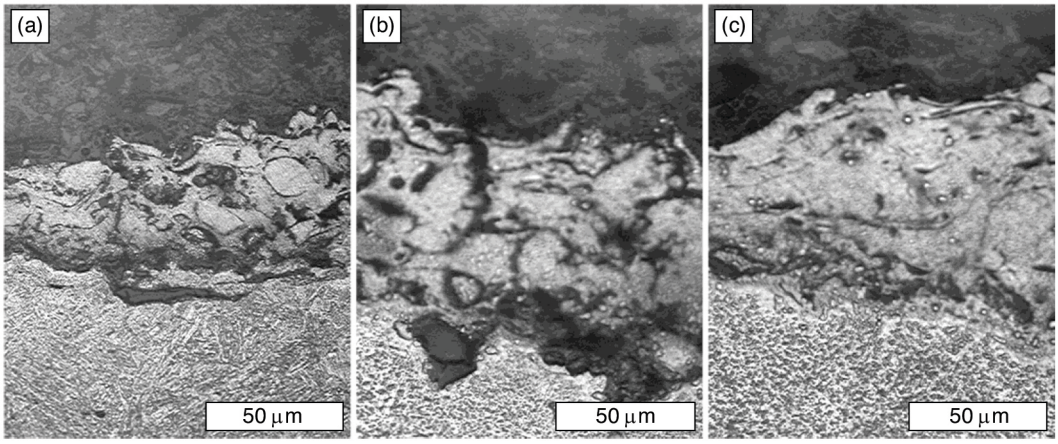

Figure 6. Microstructure (OM, etched) of the NiCr-Al-Co-Y_2O_3 / ZrO_2-MgO TBC system after thermal cycling testing; (a) sample 1 (after 7 cycles), (b) sample 2 (after 32 cycles), and (c) sample 3 (after 79 cycles)

to the presence of vacancies and the interconnected porosity network present within the top coat allows free flow of oxygen [20]. This promoted diffusion of the oxygen to the bond coat surface and its oxidation. Interlamellar porosity of the bond coat enabled further diffusion of the oxygen through the bond coat and its reaction with Al, Ni, Cr, and Co, which was confirmed with the later EDS analysis. The EDS analysis also confirmed the oxidations at 1200 °C of the chemical elements in γ-Ni(Cr) solid solution, which diffuse toward the bond coat surface.

The EDS analysis of the NiCr-Al-Co-Y_2O_3 bond coat after thermal cycling testing (sample 1, sample 2, and sample 3) is performed on SEM images. For sample 1 (after 7 cycles) only one EDS analysis is performed in the γ-Ni(Cr) solid solution region, near to the top coat, while for sample 2 (after 32 cycles), and sample 3 (after 79 cycles) two EDS analysis are performed, *i.e.* EDS 1 and EDS 2. The EDS 1 is performed in the oxide region, near to the top coat, and EDS 2 in the γ-Ni(Cr) solid solution region, near to the substrate. For the purpose of easier comparison, all EDS analysis results are summarised in one table, tab. 5.

Table 5. Chemical composition of the bond coat samples before and after thermal cycling testing, wt.%

Element	As-deposited	After 7 cycles	After 32 cycles		After 79 cycles	
	EDS	EDS	EDS 1	EDS 2	EDS 1	EDS 2
O	–	–	27.45	–	29.48	–
Al	1.11	0.98	22.60	6.12	26.75	5.75
Cr	22.82	19.33	9.11	38.55	17.93	17.85
Fe	–	–	0.89	8.34	2.48	15.70
Co	3.88	2.93	0.97	3.29	1.03	2.63
Ni	72.19	76.76	29.87	43.70	9.84	58.07
Y	–	–	9.11	–	12.49	–

For sample 1 (after only 7 cycles) the EDS analysis of the γ-Ni(Cr) solid solution in the region near to the substrate was not performed, since the number of cycles was too small to affect the composition of bond coat in that region. Nevertheless, the performed EDS analysis of the sample 1, fig. 7, showed that the chemical composition of NiCr-Al-Co-Y_2O_3 coating after 7 cycles differs from the chemical composition of as-deposited NiCr-Al-Co-Y_2O_3 coating, fig. 3. This change is the result of Al, Cr, and Co diffusion at 1200 °C, toward the bond coat surface. Hence, the amount of Al, Cr and Co in the region near to the top coat is lower after 7 cycles comparing to as-deposited state.

Microstructure of the bond coat bond coat after 32 cycles (sample 2) and corresponding EDS analysis results are shown in fig. 8. Appearance of the first horizontal (parallel and close to the bond coat/top coat interface) cracks in the ceramic ZrO_2-MgO top coat, as well as vertical cracks through the bond coat, could be noticed. Due to the increased number of thermal cycles in sample 2, which accelerate the diffusion of oxygen through the bond coat and the diffusion of chemical elements in γ-Ni(Cr) solid solution toward the bond coat surface, there has been a major change in the chemical composition of bond coat in comparison with the state after 7 thermal cycles or the as-deposited state, tab. 5.

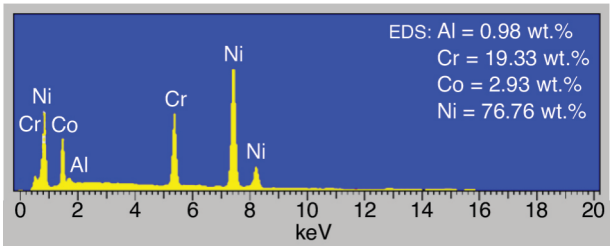

Figure 7. The EDS analysis results of the NiCr-Al-Co-Y_2O_3 bond coat after 7 cycles (sample 1)

The EDS analysis (EDS 1) of the oxide region, near to the top coat, shows accelerated diffusion of Al, Ni, Cr, and Co from the γ-Ni(Cr) solid solution toward the bond coat surface, and their oxidation. The NiO, CoO, and Cr_2O_3 oxides are unstable at 1200 °C, so they interreacted and formed more stable oxides. Presence of Fe (0.89 wt.%) was also noticed in EDS 1 region. This Fe diffused from the substrate toward the bond coat surface and most probably, due to the reaction with oxygen, formed Fe_2O_3 oxide as well [21]. The EDS analysis (EDS 2) of the γ-Ni(Cr) solid solution region, near to the substrate, shows increased amount of Fe (8.34 wt.%), that diffused from the substrate. On the other hand, the amount of Ni is lower, most probably due to the diffusion of Ni into the substrate.

Microstructure of the bond coat bond coat after 79 cycles (sample 3) and corresponding EDS analysis results are shown in fig. 9. Horizontal (parallel and close to the bond coat/top coat interface) cracks in the ceramic ZrO_2-MgO top coat, as well as vertical cracks through the bond coat, could be clearly noticed. These horizontal cracks are one of the main reasons for the failure

of TBC systems exposed to thermal cycling, *i.e.* delamination of ceramic top coat [7, 8]. They were caused by stresses arising from the thermal mismatch between the metallic bond coat and the ceramic top coat. However, the thermal cycling is not only a process for the accumulation of internal stress, but also a process that causes fatigue of the oxide layer, which would affect the thermal cyclic lifetime of TBCs [22]. Due to the increased number of thermal cycles, amount of oxides in bond coat increases, leading to the decrease of bond coat ductility. Hence, the formation of the vertical cracks through the bond coat is more intensive.

The change in chemical composition of bond coat, in comparison with the as-deposited state, tab. 5, was the biggest with the sample 3, *i.e.* after 79 cycles. The EDS analysis (EDS 1) of the oxide region, near to the top coat, shows that the diffusion of Al, Ni, Cr, and Co from the γ-Ni(Cr) solid solution, toward the bond coat surface, was the most intensive in sample 3. The diffusion of Fe from the substrate was also more intensive, and its amount was higher in EDS 1 region of sample 3 (2.48 wt.%) than in the same EDS region of sample 2 (0.89 wt.%). The EDS analysis (EDS 2) of the γ-Ni(Cr) solid solution region, near to the substrate, confirmed that the diffusion of Fe from the substrate was the most intensive in sample 3, *i.e.* the amount of Fe in this region (15.70 wt.%) was the highest of all analysed regions and samples. It is interesting that the oxygen was not detected in the EDS 2 regions of samples exposed to prolonged number of thermal cycles, not even after 79 cycles. This suggests that the formed complex oxides of the Al_2O_3-Y_2O_3 dual system, formed during deposition and during thermal cycling testing, successfully protected substrate from the oxidation.

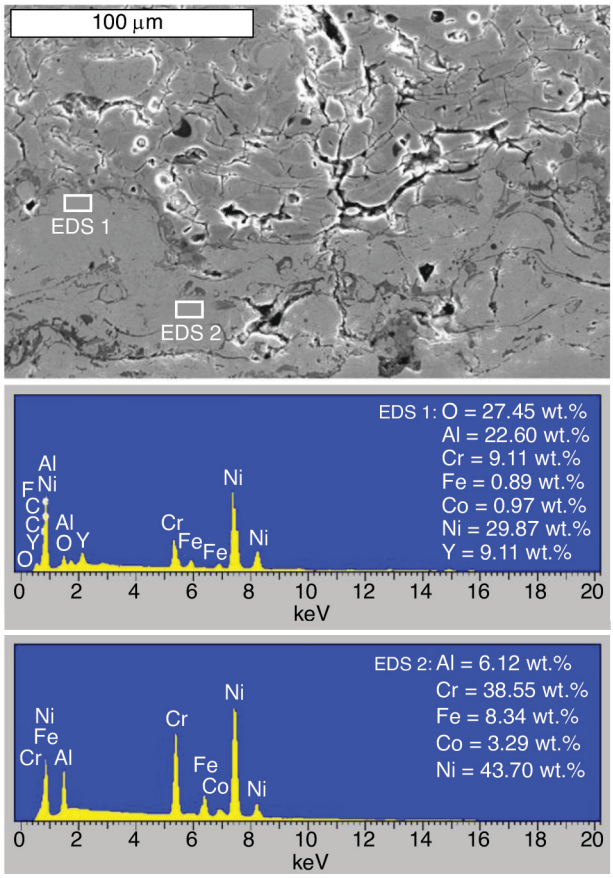

Figure 8. Microstructure (SEM, polished) of the NiCr-Al-Co-Y_2O_3 bond coat after 32 cycles (sample 2) and corresponding EDS analysis results

The obtained values of microhardness for bond coat (NiCr-Al-Co-Y_2O_3) samples after thermal cycling testing are shown in fig. 4. The values of microhardness of all samples were higher after the thermal cycling testing, than the values of as-deposited samples. The microhardness values of tested samples increase as the number of cycles increase, and the highest value showed sample 3 (after 79 cycles). This is a consequence of prolonged exposure of samples to high temperature (1200 °C). At this temperature, diffusion of oxygen from air and iron from steel substrate to the bond coat, occurs [7, 21], which is confirmed with the microstructural analysis. The diffused elements formed oxides, increasing the bond coat hardness.

The influence of thermal cycling on microhardness is analysed through the influence of number of cycles on the increase of microhardness, fig. 10. This comparison is very useful, since the ambient temperature mechanical properties values do not necessarily provide an indicator of the relative high temperature properties [8]. The calculated percentage increase of microhardness of tested samples is in good, linear correlation with the number of cycles during the thermal cycling testing.

Conclusions

The microstructure of as-deposited NiCr-Al-Co-Y_2O_3 bond coat was uniform lamellar structure with negligible amount of unmelted particles, and without the presence of micro or macro cracks. It contained lamellar nickel-chrome particles of a γ-Ni(Cr) solid solution and thin lamellar α-Al_2O_3 oxides and complex oxides $YAlO_3$ (YAP) and $Y_3Al_5O_{12}$ (YAG) of the Al_2O_3-Y_2O_3 dual system, evenly distributed between the nickel-chrome lamellas. The smaller amount of Al in the γ-Ni(Cr) solid solution lamellas indicated that most of the Al reacted with oxygen from the air and with Y_2O_3 from the powder, during the deposition.

Thermal cycling testing at 1200 °C affected the bond between bond coat and substrate, but the delamination of the coating was not noticed on any sample, not even on samples exposed to prolonged number of thermal cycles. The diffusion of Al, Ni, Cr, and Co from the γ-Ni(Cr) solid solution, and Fe from the steel substrate toward the bond coat surface, and their oxidation occurred due to the high temperature. Nevertheless, the formation of brittle TGO layer was not noticed on any thermally cycled sample. Instead of more brittle α-Al_2O_3 TGO layer, complex oxides of the Al_2O_3-Y_2O_3 dual system minimised the diffusion of oxygen during thermal cycling testing. These complex oxides,

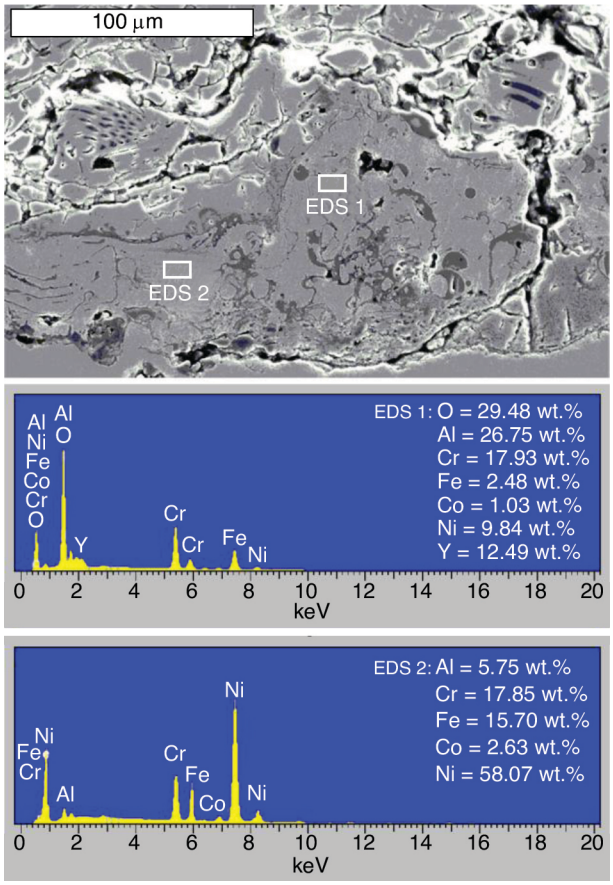

Figure 9. Microstructure (SEM, polished) of the NiCr-Al-Co-Y_2O_3 bond coat after 79 cycles (sample 3) and corresponding EDS analysis results

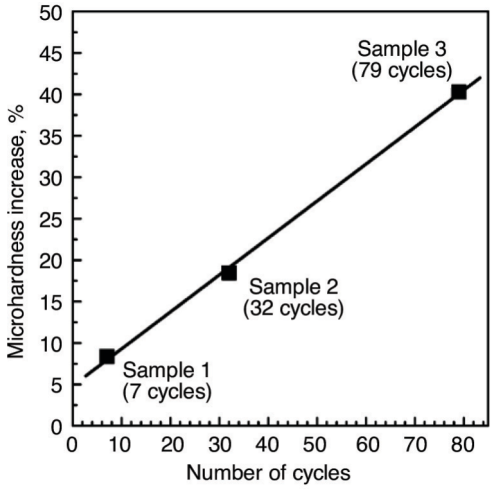

Figure 10. Microhardness increase *vs.* number of cycles during the thermal cycling testing

formed during deposition and during thermal cycling testing, successfully protected substrate from the oxidation.

Preheating of the substrate induced higher microhardness and higher tensile bond strength of the as-deposited bond coat, which were in correlation with the microstructural analysis. The values of microhardness of all samples were higher after the thermal cycling testing, than the values of as-deposited samples, due to the diffusion of oxygen from air and iron from steel substrate to the bond coat, and formation of oxides. The correlation between the number of cycles and increase of microhardness of tested samples were linear.

Acknowledgement

This work has been performed as a part of activities within the projects TR 34028, TR 35021 and OI 174004. These projects are supported by the Republic of Serbia, Ministry of Education, Science and Technological Development, whose financial help is gratefully acknowledged.

References

[1] Wortman, D. J., *et al*., Thermal Barrier Coatings for Gas Turbine Use, *Materials Science and Engineering A*, *120-121* (1989), 2, pp. 433-440
[2] Stover, D., Funke, C., Directions of the Development of Thermal Barrier Coatings in Energy Applications, *Journal of Materials Processing Technology*, *92-93* (1999), Aug., pp. 195-202
[3] Vaßen, R., *et al*., Advanced Thermal Spray Technologies for Applications in Energy Systems, *Surface and Coatings Technology*, *202* (2008), 18, pp. 4432-4437
[4] Durat, M., *et al.*, The Effects of Coating Materials in Spark Ignition Engine Design, *Materials & Design*, *36* (2012), Apr., pp. 540-545
[5] Ramalingam, S., *et al*., Application of Thermal Barrier Coating for Improving the Suitability of Annona Biodiesel in a Diesel Engine, *Thermal Science*, *20* (2016), Suppl., pp. S973-S979
[6] Peng, X., Metallic Coatings for High-Temperature Oxidation Resistance, in: *Thermal Barrier Coatings* (Eds. H. Xu, H. Guo), Woodhead Publishing Limited, Cambridge, UK, 2011, pp. 53-74
[7] Mrdak, M. R., *et al*., Influence of Plasma Spraying Parameters on Properties of the Thermal Barrier Coatings, *Materials Science and Technology*, *29* (2013), 5, pp. 559-567
[8] Haynes, J. A., *et al*., Thermal Cycling Behavior of Plasma-Sprayed Thermal Barrier Coatings with Various MCrAlX Bond Coats, *Journal of Thermal Spray Technology*, *9* (2000), 1, pp. 38-48
[9] Zhou, C. G. Song, Y. X., Oxidation and Hot Corrosion of Thermal Barrier Coatings (TBCs), in: *Thermal Barrier Coatings* (Eds. H. Xu, H. Guo), Woodhead Publishing Limited, Cambridge, UK, 2011, pp. 193-214
[10] Yuan, F. H., *et al*., Oxidation Behavior of Thermal Barrier Coatings with HVOF and Detonation-Sprayed NiCrAlY Bondcoats, Corrosion Science, *50* (2008), 6, pp. 1608-1617
[11] Saeidi, S., Microstructure, Oxidation & Mechanical Properties of As-Sprayed and Annealed HVOF & VPS CoNiCrAlY Coatings, Ph. D. thesis, University of Nottingham, Nottingham, UK, 2010
[12] Eriksson, R., *High-Temperature Degradation of Plasma Sprayed Thermal Barrier Coating Systems*, Linkoping University Electronic Press, Linkoping, Sweden, 2011
[13] Medraj, M., *et al*., High Temperature Neutron Diffraction Study of the Al2O3-Y2O3 System, *Journal of the European Ceramic Society*, *26* (2006), 16, pp. 3515-3524
[14] ***, Metco 461 Nickel Chromium-Aluminum-Cobalt-Yttria Composite Powder, Technical Bulletin 10-315, Sulzer Metco, Switzerland, 2000
[15] ***, Metco 210 Magnesium Zirconate Powder, Technical Bulletin 10-108, Sulzer Metco, Switzerland, 2000
[16] ***, Turbojet Engine - Standard Practices Manual (PN 582005), Pratt & Whitney, East Hartford, USA, 2002
[17] Wojewoda-Budka, J., *et al*., Interactions between Molten Aluminum and Y_2O_3 Studied with TEM Techniques, *Journal of Microscopy*, *237* (2010), 3, pp. 253-257
[18] Fabrichnaya, O., *et al*., The Assessment of Thermodynamic Parameters in the Al_2O_3-Y_2O_3 System and Phase Relations in the Y-Al-O System, *Scandinavian Journal of Metallurgy*, *30* (2001), 3, pp. 175-183
[19] Vencl, A., *et al.*, Evaluation of Adhesion/Cohesion Bond Strength of the Thick Plasma Spray Coatings by Scratch Testing on Coatings Cross-Sections, *Tribology International*, *44* (2011), 11, pp. 1281-1288
[20] Gupta, M., *Design of Thermal Barrier Coatings*, Springer, Cham, Switzerland, 2015

[21] Zhu, C., *et al*., The Effect of Initial Oxidation on Long-Term Oxidation of NiCoCrAlY Alloy, *Engineering*, *2* (2010), 8, pp. 602-607
[22] Zhang, D., Thermal Barrier Coatings Prepared by Electron Beam Physical Vapor Deposition (EB–PVD), in: *Thermal Barrier Coatings* (Eds. H. Xu, H. Guo), Woodhead Publishing Limited, Cambridge, UK, 2011, pp. 3-24

Paper submitted: March 2, 2018
Paper revised: September 10, 2019
Paper accepted: September 12, 2019